

Broadband dispersion-free optical cavities based on zero group delay dispersion mirror sets

Li-Jin Chen,^{1,*} Guoqing Chang,¹ Chih-Hao Li,² Andrew J. Benedick,¹ David F. Phillips,² Ronald L. Walsworth,² and Franz X. Kärtner¹

¹Research Laboratory of Electronics, Massachusetts Institute of Technology, Cambridge, MA 02139, USA

²Harvard-Smithsonian Center for Astrophysics, Harvard University, Cambridge MA 02138, USA

*lijinc@mit.edu

Abstract: A broadband dispersion-free optical cavity using a zero group delay dispersion (zero-GDD) mirror set is demonstrated. In general zero-GDD mirror sets consist of two or more mirrors with opposite group delay dispersion (GDD), that when used together, form an optical cavity with vanishing dispersion over an enhanced bandwidth in comparison with traditional low GDD mirrors. More specifically, in this paper, we show a realization of such a two-mirror cavity, where the mirrors show opposite GDD and simultaneously a mirror reflectivity of 99.2% over 100 nm bandwidth (480 nm – 580 nm).

©2010 Optical Society of America

OCIS codes: (310.4165) Multilayer design; (050.2230) Fabry-Perot; (230.4040) Mirrors.

References and links

1. F. X. Kärtner, U. Morgner, R. Ell, T. Schibli, J. G. Fujimoto, E. P. Ippen, V. Scheuer, G. Angelow, and T. Tschudi, "Ultrabroadband double-chirped mirror pairs for generation of octave spectra," *J. Opt. Soc. Am. B* **18**(6), 882–885 (2001).
2. V. Pervak, A. V. Tikhonravov, M. K. Trubetskov, S. Naumov, F. Krausz, and A. Apolonski, "1.5-octave chirped mirror for pulse compression down to sub-3 fs," *Appl. Phys. B* **87**(1), 5–12 (2007).
3. T. Udem, R. Holzwarth, and T. W. Hänsch, "Optical frequency metrology," *Nature* **416**(6877), 233–237 (2002).
4. C. Gohle, T. Udem, M. Herrmann, J. Rauschenberger, R. Holzwarth, H. A. Schuessler, F. Krausz, and T. W. Hänsch, "A frequency comb in the extreme ultraviolet," *Nature* **436**(7048), 234–237 (2005).
5. M. J. Thorpe, K. D. Moll, R. J. Jones, B. Safdi, and J. Ye, "Broadband cavity ringdown spectroscopy for sensitive and rapid molecular detection," *Science* **311**(5767), 1595–1599 (2006).
6. Z. Jiang, D. E. Leaird, and A. M. Weiner, "Line-by-line pulse shaping control for optical arbitrary waveform generation," *Opt. Express* **13**(25), 10431–10439 (2005).
7. C. H. Li, A. J. Benedick, P. Fendel, A. G. Glenday, F. X. Kärtner, D. F. Phillips, D. Sasselov, A. Szentgyorgyi, and R. L. Walsworth, "A laser frequency comb that enables radial velocity measurements with a precision of 1 cm s⁻¹," *Nature* **452**(7187), 610–612 (2008).
8. T. Steinmetz, T. Wilken, C. Araujo-Hauck, R. Holzwarth, T. W. Hänsch, L. Pasquini, A. Manescau, S. D'Odorico, M. T. Murphy, T. Kentscher, W. Schmidt, and T. Udem, "Laser frequency combs for astronomical observations," *Science* **321**(5894), 1335–1337 (2008).
9. D. A. Braje, M. S. Kirchner, S. Osterman, T. M. Fortier, and S. A. Diddams, "Astronomical spectrograph calibration with broad-spectrum frequency combs," *Eur. Phys. J. D* **48**(1), 57–66 (2008).
10. J. R. Birge, and F. X. Kärtner, "Efficient optimization of multilayer coatings for ultrafast optics using analytic gradients of dispersion," *Appl. Opt.* **46**(14), 2656–2662 (2007).
11. A. J. Benedick, G. Chang, J. R. Birge, L.-J. Chen, A. G. Glenday, C.-H. Li, D. F. Phillips, A. Szentgyorgyi, S. Korzennik, G. Furesz, R. L. Walsworth, and F. X. Kärtner, "Visible wavelength astro-comb," *Opt. Express* **18**(18), 19175–19184 (2010).
12. G. Chang, L.-J. Chen, and F. X. Kärtner, "Highly efficient Cherenkov radiation in photonic crystal fibers for broadband visible wavelength generation," *Opt. Lett.* **35**(14), 2361–2363 (2010).
13. A.-C. Tien, S. Backus, H. Kapteyn, M. Murnane, and G. Mourou, "Short-Pulse Laser Damage in Transparent Materials as a Function of Pulse Duration," *Phys. Rev. Lett.* **82**(19), 3883–3886 (1999).
14. F. Gori, and G. Guattari, "Bessel-Gauss Beams," *Opt. Commun.* **64**(6), 491–495 (1987).
15. W. P. Putnam, G. Abram, E. L. Falcão-Filho, J. R. Birge and F. X. Kärtner, "High-Intensity Bessel-Gauss Beam Enhancement Cavities," CLEO/QELS 2010, paper CMD1.

1. Introduction

Dielectric coatings with custom reflectivity and group-delay dispersion (GDD) over a desired spectral range are key components in ultrafast optics. With powerful computer-based optimization algorithms, one can explore a multi-dimensional design space (constructed by the choice of material and layer thickness) and create sophisticated coating designs for the manipulation of laser pulses of various durations and spectral coverage. For example, incorporation of broadband double-chirped mirrors (DCMs) into mode-locked Ti:sapphire lasers for precise GDD compensation has been used for achieving octave-spanning spectra directly from a laser cavity [1]. Compression of ultrabroadband laser pulses down to sub-two cycles using dispersion-compensating mirrors with a bandwidth spanning over 1.5 octaves has been recently demonstrated [2]. With both their pulse repetition rate and carrier-envelope phase stabilized, these lasers become frequency combs, whose spectra are composed of many narrow and equally spaced optical lines. In addition to precision frequency metrology [3], frequency combs have found more applications via short pulse field enhancement or repetition-rate multiplication with the aid of high-finesse optical cavities. For short pulse field enhancement, the equally-spaced spectral lines of a frequency comb are coupled into a cavity with a free-spectral range (FSR) matched to the laser pulse repetition rate, which constructively enhances the resonant pulse circulating inside the cavity without the need of active amplification. This enhancement technique has been used in the facilitation of high harmonic generation driven by high repetition-rate (i.e. ~ 100 MHz) lasers, enabling the generation of EUV frequency combs [4]. If gaseous samples are introduced into the cavity, the effective interaction length between light and sample can be increased by many orders of magnitude, leading to an unprecedented high sensitivity in spectroscopy [5]. For repetition-rate multiplication, the cavity FSR is tuned to be an integer multiple of the source-comb spectral line spacing and the cavity acts as a filter that selectively suppresses unwanted lines and passes those aligned with the cavity's narrow transmission resonances. The resulting filtered comb can be spatially resolved by spectral dispersers so that individual spectral lines become accessible and controllable. Rarely achieved from fundamentally mode-locked solid-state lasers, such high repetition-rate sources are essential for many applications such as arbitrary optical waveform generation through line-by-line modulation [6] and precision wavelength calibration of astrophysical spectrographs for the detection of Earth-analogous extra-solar planets (the resulting filtered comb is often called an astro-comb) [7–9].

One crucial requirement of the optical cavity is to have wavelength independent FSR, or equivalently wavelength independent round trip optical length over a broad bandwidth to ensure that the frequencies of the transmission resonances are aligned with equally-spaced frequency comb lines, which can be achieved by designing a broadband zero-dispersion cavity. For short pulse field enhancement, the cavity bandwidth limits the transform-limited pulse duration as well as the peak intensity of the circulating pulses. In the astrophysical spectrograph calibration, the cavity bandwidth limits the available wavelength coverage and thus compromises the calibration accuracy. Currently, most of the enhancement or filter cavities are constructed from dielectric mirrors that are individually designed to have negligible dispersion or compensate the GDD of intracavity materials at a certain wavelength range. In this paper, we demonstrate a novel design for an optical cavity that consists of a set of dielectric mirrors with zero GDD in reflection, which allows optimization of many mirrors simultaneously to extend cavity bandwidth. The design concept, optimization algorithm, and tolerance to manufacturing errors for such zero-GDD mirror sets are also discussed. As an example, we present our design and experimental demonstration of the first zero-GDD mirror pair with 100-nm bandwidth (480–580 nm) and $\sim 99.2\%$ reflectivity using $\text{Nb}_2\text{O}_5/\text{SiO}_2$ layer pairs. This mirror pair is designed for construction of a Fabry-Perot (FP) filter cavity with 40 GHz FSR, a pivotal device for implementing a broadband astro-comb in the visible

wavelength range. The demonstrated cavity, for the first time, has successfully transformed a 1 GHz green comb into an astro-comb spanning over 100nm bandwidth.

2. Design concepts

As a linear closed-loop system, a passive optical cavity can be modeled in a lumped way with its loop transfer function $H(\omega)$ determined by all cavity mirrors and intracavity materials per round-trip. The magnitude $|H(\omega)|$ is the accumulated amplitude decay ratio and the phase shift $\varphi(\omega) = \angle H(\omega)$. Assuming that an input field is coupled into the cavity and propagating to a certain reference plane, the power spectrum of the circulating pulse at that plane is scaled by the following closed-loop transfer function:

$$\left| \frac{1}{1 - |H(\omega)| e^{j\varphi(\omega)}} \right|^2 \quad (1)$$

For a passive high-finesse cavity, $|H(\omega)|$ is close to but less than one. Inside the cavity, resonant frequencies, corresponding to $\varphi(\omega)$ being a multiple of 2π , are significantly enhanced. From a simple physical viewpoint, this phase shift originates from the required round-trip time for the light at a certain wavelength. When the round-trip time is wavelength-independent, $\varphi(\omega)$ becomes simply a linear function of ω . Therefore, the resulting resonances are equally spaced in the frequency domain. By careful adjustment of the cavity length and eventually also the carrier-envelope offset frequency of the laser, these resonant frequencies can be tuned to align with frequency comb lines. However, due to the cavity dispersion, the non constant mode spacing causes a mismatched cavity. The tolerance against residual dispersion depends on the cavity finesse. As $|H(\omega)|$ approaches a high finesse cavity, i.e. $|H(\omega)| \rightarrow 1$, the closed loop transfer function is more sensitive to the phase, and the resulting tolerance to dispersion-induced deviations in mode spacing caused by phase deviations becomes smaller. In other words, even a small phase deviation from a multiple of 2π can lead to a dramatic decrease in the cavity's transmission for frequencies around resonances. One can derive a simple criterion for estimating this phase tolerance by solving for the phase corresponding to half of the maximum of (1) and find:

$$\phi(\omega) < \frac{1 - |H(\omega)|}{\sqrt{|H(\omega)|}} \approx 1 - |H(\omega)|, \text{ for } |H(\omega)| \approx 1 \quad (2)$$

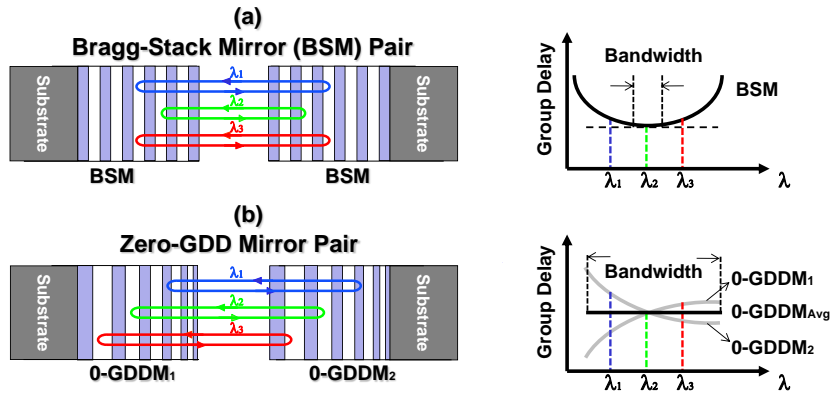


Fig. 1. Schematic of the two-mirror dispersion-free cavity based on (a) Bragg-stack mirror pair and (b) zero-GDD mirror pair. The curves on the right show the individual and average group delay on the cavity mirrors as a function of wavelength.

For example, to design a dispersion-free Fabry-Perot cavity consisting of two identical mirrors with a reflectivity of 99% ($|H(\omega)| = \sqrt{0.99 \times 0.99}$), one needs to ensure the dispersion-induced phase deviation is less than 0.01 radian within the desired wavelength range. For applications demanding less distortion on the filtered comb lines, this value could be even smaller.

In the traditional cavity designs, low-dispersion mirrors based on Bragg-stack mirrors (BSMs) are commonly used, as shown in Fig. 1(a). Although BSMs are typically high reflectors with a moderate bandwidth, different wavelengths reflect from different depths inside the structure. Consequently, only a narrow spectral range near the center of the high-reflectivity region experiences negligible dispersion, imposing limitations on effective cavity bandwidth. In practice, slight optimization is usually required to broaden the usable bandwidth of such BSM-based, low-dispersion mirrors, but the possible improvement is very limited. In addition, any uncompensated dispersion from intracavity materials causes further bandwidth narrowing. As a result, it is often necessary to put the cavity in vacuum to avoid air dispersion. In this sense, any individual component with non-zero dispersion is limiting the cavity bandwidth. However, the real bottleneck, as discussed earlier, is the cavity round-trip time. A constant round-trip time for the wavelengths of interest does not imply that they have to travel at the same speed. Instead, as we will show in the following sections, allowing some dispersion on the mirror coating provides additional degrees of freedom to design cavity mirror sets for broadband cavities. This idea is illustrated in Fig. 1(b) with a simple mirror pair shown as an example. Note that the concept can be easily generalized to a mirror set including even more mirrors. As plotted in the figure, the layer thicknesses of the mirror pair are chirped to create a complementary, wavelength-dependent penetration depth in both mirror coatings. With the total dispersion minimized, such a mirror pair constitutes a dispersion-free building block for optical cavities. Compared to individually-optimized BSM cavities, this approach excels because chirped-mirrors intrinsically have larger bandwidth and more flexibility for dispersion customization, which creates a larger parameter space for extending the bandwidth of dispersion-free cavities. Another advantage of optimizing a mirror set instead of individual mirrors is that the intracavity material dispersion can be easily taken into account in the design process. For a complicated multi-mirror cavity, mirror sets can even be designed to provide additional features such as transmission windows at specific wavelengths to meet the application requirements. Eventually, the cavity can use one or more zero-GDD mirror sets with all the necessary features without significant bandwidth reduction. In short, zero-GDD mirror sets are a set of mirrors jointly optimized to provide custom reflectivity and negligible dispersion over a large bandwidth. Also, depending on the application, additional characteristics can be implemented during the design process.

3. Optimization algorithm and design issues

The design of a zero-GDD mirror set is based on the efficient group-delay (GD) computation approach developed in Ref. 10. The optimum layer thicknesses are found by minimizing the merit function that evaluates the weighted deviation of the computed dispersion and reflectivity from our design goal. The wavelength range of interest is discretized into k points, denoted as λ_k . The employed merit function is simply determined by the summation of the weighted deviation from the targeted reflectivity and GD values corresponding to the thicknesses of the layer set x :

$$f(x) = \sum_k \left\{ \omega_R(\lambda_k) \left[R(\lambda_k; x) - R_{goal}(\lambda_k) \right]^4 + \omega_d(\lambda_k) \left[\tau_g(\lambda_k; x) - \tau_{g,goal}(\lambda_k) + \tau_{g0}(x) \right]^2 \right\} \quad (3)$$

where R is the reflectivity, τ_g the group delay, and $\omega_{R,d}$ the weighting function for the reflectivity and GD goals. The term τ_{g0} is used to exclude the irrelevant offset between the

computed and ideal GD, which minimizes $f(x)$ for a given layer set x . To find good initial structures to start with, we first optimize all mirrors separately using smooth GD functions split from a GD goal that is complementary to the dispersion of the materials. This ensures that the remaining errors are mostly from higher-order dispersion. In the second step the residual dispersion is minimized with an iterative optimization procedure in which all the mirrors are optimized in turns. The requirement of a constant round-trip time is implemented in this step by updating the GD goal of the mirror to be optimized with the computed GD of all other mirrors and the materials:

$$\tau_{g,goal}^k(\lambda_k) = -\sum_{i \neq k} \tau_g^i(\lambda_k; x^i) - \tau_g^{material}(\lambda_k) \quad (4)$$

The iteration continues until the target specification is reached.

Theoretically, an ultrabroadband (e.g., 650-1100nm) zero-GDD mirror set can be produced using this algorithm by designing a complementary double-chirped mirror pair [1], with one mirror having the opposite average dispersion of the other one. In practice, broadband highly dispersive mirror designs demand higher precision in fabrication, a requirement ultimately limited by the capability of current coating technology. The increased sensitivity stems simply from the increased penetration depth of the light into the mirror giving rise to spurious reflections [1]. The deeper the penetration the more opportunity there is for such reflections to occur. As a result, it is always necessary to confirm the robustness of a practical design by adding random thickness perturbations to each layer, imitating manufacturing errors; and to estimate the resulting phase errors for worst-case scenarios.

4. Design examples: a two-mirror zero-GDD mirror pair for green (480-580 nm) filtering cavities

To demonstrate the idea, we have designed a zero-GDD mirror set consisting of a complementary mirror pair supporting a dispersion-free region from 480 to 580 nm. This zero-GDD pair is aimed for a moderate-finesse (>250) FP filtering cavity, as used in a green astro-comb. Astro-combs that cover spectral bands in the green (480 nm – 580 nm) are of particular interest in high accuracy astronomical spectroscopy because this wavelength region provides the largest photon flux from sun-like stars and is rich in spectral features of high quality. Charge-coupled devices (CCDs) used in astrophysical spectrograph also have better response in this wavelength region. Recently, we have demonstrated a blue astro-comb (410 nm – 425 nm) [11] based on a frequency-doubled 1 GHz Ti:sapphire frequency comb filtered by a FP cavity. Limited by the bandwidth of the phase matching of the frequency doubling process in a 1 mm thick beta-barium borate (BBO) crystal, the blue astro-comb has a bandwidth of only 15 nm, which is slight narrower than the transmission bandwidth of the FP cavity (20nm) made with two identical, individually-optimized low-dispersion mirrors. In order to design more powerful astro-combs that span much larger bandwidths using our recently-developed broadband visible source [12], we constructed a broadband dispersion-free cavity using a zero-GDD mirror pair. Figure 2 shows the calculated reflectivity and group delay of the zero-GDD mirror pair designed for a ~ 40 GHz FSR cavity. The dispersion caused by 7.5 mm of intracavity air (~ 0.24 fs² for 1 atmosphere at 300 K) is taken into account during the optimization. With an initial structure of 22 layers of Nb₂O₅/SiO₂ quarter-wave layer pairs, both mirrors are optimized to have a reflectivity of $\sim 99.2\%$ and complementary dispersion over the desired range [Fig. 2 (a)], which supports a FP filtering cavity with a finesse of ~ 390 . For comparison, we also designed a similar low-dispersion mirror centered at 530 nm based on the traditional approach, i.e. individually-optimized BSMs [Fig. 2(b)]. In Fig. 2(c), we compare the calculated total GD of the FP cavities built with both designs and find a three-fold bandwidth improvement with the new zero-GDD mirror set design even when the traditional design is evaluated for a cavity in vacuum. Such improvement is due to the simultaneous optimization of the mirrors of the zero-GDD set.

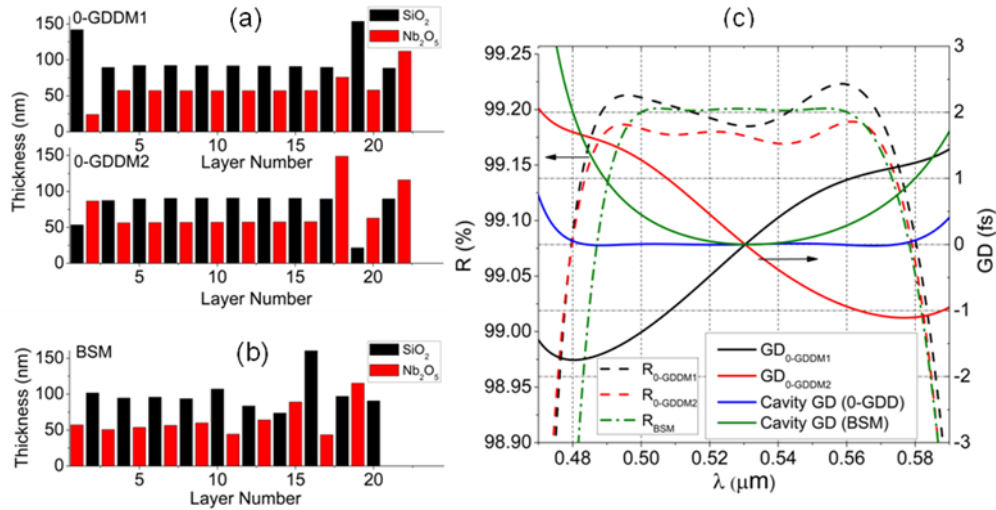


Fig. 2. (a) Structure of a two-mirror zero-GDD mirror set designed for a 40GHz FSR, 100 nm bandwidth (480-580 nm) cavity using Nb₂O₅/SiO₂ layer pairs. (b) Structure of a low-dispersion BSM mirror that is individually optimized for the same goal. (c) Calculated reflectivity (dotted curves) and group delay (solid curves) of the zero-GDD mirror pair. The total cavity group delay using the zero-GDD mirror pair (blue) is calculated by taking the dispersion of both mirrors and 7.5 mm of air into account. As a comparison, the total GD (solid) and reflectivity (dashed) of a cavity in vacuum based on two individually-optimized, low-dispersion BSMs is shown in green.

As mentioned in the previous section, the bandwidth can be even larger if the structures are more chirped. However, this will inevitably degrade the manufacturability of the mirrors and causes uncertainty for astro-comb applications that demand extremely low phase error. As a result, we used quarter-wave layer pairs, identical to the traditional design, as the initial structure for optimizing the zero-GDD mirror set, a conservative design that improves robustness to manufacturing errors. Figure 3(a) illustrates the simulated phase deviation from a zero-dispersion cavity using the zero-GDD mirror pair shown in Fig. 2(a) with manufacturing thickness errors taken into account. The analysis is performed with 100 tests assuming random layer thickness fluctuations of ± 0.5 nm on each layer of both mirrors. The spread of possible round-trip phase errors confirms that the criterion (2) is fulfilled in the presence of reasonable manufacturing tolerances.

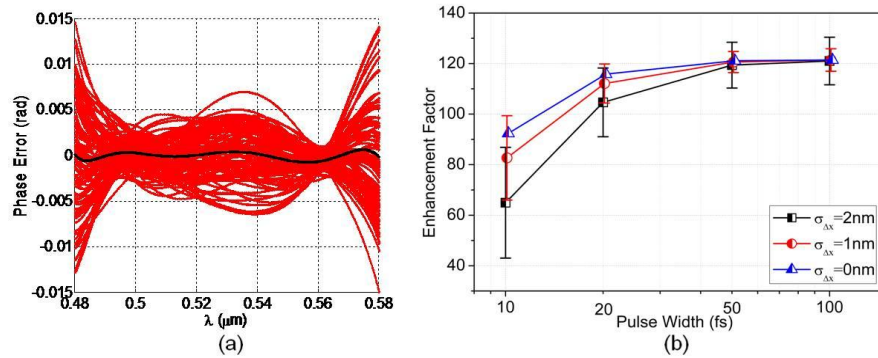


Fig. 3. (a) Simulated phase deviation from a dispersion-free cavity using one zero-GDD mirror pair. The deviation of the ideal zero-GDD mirror pair design is shown in black and the spread of possible phase errors with 100 tests assuming a random manufacturing error of ± 0.5 nm for the mirror layer thicknesses is shown in red. (b) Estimated enhancement factors for 100, 50, 20 and 10 fs Gaussian pulses considering normally-distributed manufacturing errors with a standard deviation σ_x of = 0 (blue), 1 (red), and 2 nm (black). Each marker indicates shows the average value and the error bar shows the standard deviation of enhancement factor for 1000 tests.

We also performed another analysis on our zero-GDD mirror pair to show that it can also be applied to broadband pulse enhancement in the few-cycle pulse regime. We simulated the enhancement factor for 100, 50, 20 and 10 fs Gaussian pulses with the central wavelength matched to the cavity. Normally-distributed random thickness errors with a standard deviation σ_x of 0, 1, and 2 nm were added to each layer. The enhancement factor was obtained by calculating the peak intensity of the steady-state intracavity pulse normalized to the input pulse. With 1000 tests on each combination of pulse duration and manufacturing tolerances, we obtained the average enhancement factor and its standard deviation [Fig. 3(b)]. The result clearly indicates that the enhancement factor approaches the theoretical limit even for relatively low accuracy in fabrication ($\sigma_x = 2$ nm); an average enhancement factor of ~ 100 can be achieved for transform-limited pulses as short as 20 fs. For applications requiring ultra-high peak intensity from cavity-enhanced femtosecond lasers, laser-induced damage threshold (LIDT) is a critical issue. However, in the subpicosecond regime LIDT does not scale linearly with the pulse duration τ but proportional to τ^x , where $x < 0.5$ [13]. For extremely high intensity experiments, however, special cavity designs [14,15] and high damage threshold coating materials are necessary.

5. Proof-of-concept experiment

As a proof-of-concept experiment, we first constructed a tunable light source in the visible wavelength range using Cherenkov radiation from a photonic crystal fiber (PCF). When pumped by ultrashort pulses (~ 10 fs), this mechanism becomes a low-threshold nonlinear process for broadband, highly efficient optical frequency up-conversion [12]. Figure 4(a) shows the experimental setup. An octave-spanning Ti:sapphire laser operating at 1 GHz repetition rate pumped a PCF with a zero-dispersion wavelength at 710 nm (NL-1.8-710). An achromatic half-wave plate and several bounces from broadband dispersion compensating mirrors were employed to optimize the polarization and duration of the input pulses. With ~ 200 pJ of coupled pulse energy, the PCF emits in the visible wavelength range covered by the designed mirror bandwidth. Figure 4(b) shows spectra before and after a ~ 40 GHz dispersion-free filtering cavity, measured with a low-resolution spectrometer. The filtering FP cavity consisted of the zero-GDD mirror coatings on slightly wedged flat substrates for avoiding etaloning effects. The measured laser spectrum is nearly undistorted after passing through the cavity, demonstrating successful filtering over the entire bandwidth of the zero-

GDD mirror pair. The detailed spectrum (see inset plot), acquired with an optical spectrum analyzer (OSA) further confirms that the individual comb lines become resolvable after filtering. The measured linewidth of the resolved comb lines was limited by the OSA, which has a resolution of ~ 20 GHz.

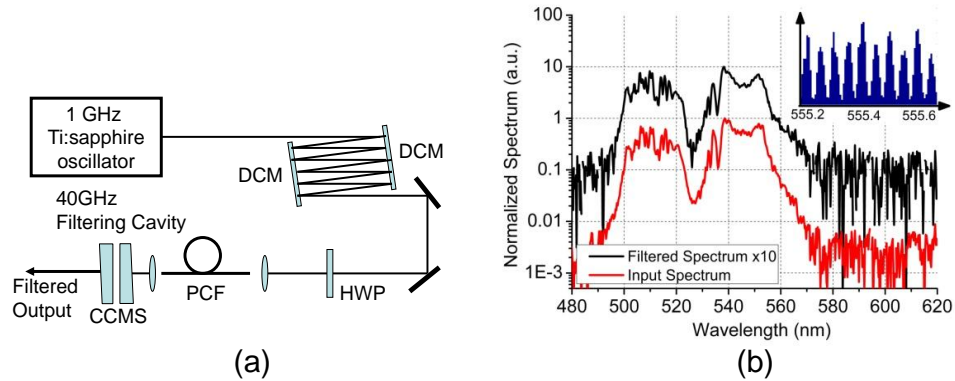


Fig. 4. (a) Experimental setup for generating a 40 GHz green astro-comb for astronomical spectrograph calibration. DCM: doubled-chirped mirrors for dispersion compensation; HWP: half-wave plate; PCF: photonic crystal fiber. (b) Input (black) and output (red) spectra before and after the 40 GHz FP filter cavity based on a zero-GDD mirror pair; inset shows detailed output spectrum near 555.4 nm obtained with a high resolution (~ 20 GHz) optical spectrum analyzer. Fluctuations of the cavity relative to the comb laser are below 5 MHz leading to an overall phase error of < 1 mrad per square root of the number of output astro-comb lines.

6. Conclusions

In conclusion, we have proposed and demonstrated a new approach for broadband dispersion-free optical cavities using a zero-GDD mirror set; e.g., to enable laser frequency combs for pulse repetition-rate multiplication and pulse enhancement. With a first zero-GDD mirror pair design, the construction of a ~ 40 GHz filtering cavity with 100 nm bandwidth for a green astro-comb (480-580 nm) was demonstrated. By proper structure scaling and re-optimization, the spectral coverage of the zero-GDD mirror set can be easily shifted to other wavelength. Further performance improvement can also be achieved by using better manufacturing techniques or materials with higher refractive index contrast since the intrinsic bandwidth of dielectric mirrors is proportional to $(n_{HL}-1)/(n_{HL} + 1)$, where n_{HL} is the ratio of higher refractive index to lower index of the dielectric materials. We believe this technique can also enable many other frequency-comb-based applications that demand large comb spacing or high peak intensity.

Acknowledgement

The authors gratefully acknowledge support from the National Science Foundation under contract AST-0905592, Defense Advanced Research Projects Agency HR0011-05-C-0155 and National Aeronautics and Space Administration under grant NNX10AE68G.